nature geoscience

LETTERS

PUBLISHED ONLINE: 29 APRIL 2012 | DOI: 10.1038/NGEO1453

Caldera size modulated by the yield stress within a crystal-rich magma reservoir

Leif Karlstrom*, Maxwell L. Rudolph and Michael Manga

The largest volcanic eruptions in the geologic record have no analogue in the historical record. These eruptions had global impacts[1,2], but are known only through their eruptive products. They have left behind calderas that formed as the surface collapsed when eruption evacuated magma chambers at 5–15 km depths[3,4]. It is generally assumed that calderas reflect the spatial dimensions of underlying magma reservoirs. Here we use a numerical model of conduit flow and dynamic magma-chamber drainage to show that caldera size can be affected by the material properties of crystal-rich silicic magma. We find that magma in the chamber can experience a rheological transition during eruption. This transition causes magma near the conduit to behave as a fluid, whereas magma farther away behaves elastically and remains locked. The intervening surface—the yield surface—expands through the chamber as eruption progresses. If a yielding transition occurs, calderas can form before complete mobilization of the entire reservoir. The resulting distribution of eruption volumes is then bimodal, as observed in the geologic record. We suggest that the presence or absence of a magma yield stress determines whether caldera size reflects the true spatial extent of magma storage.

Magma chambers function both as repositories for melt rising through the crust and as reservoirs that feed individual volcanic eruptions. During silicic caldera-forming eruptions, these functions occur on vastly different timescales as many cubic kilometres of magma gradually assembled and maintained at high crystal fraction[5] in the crust are probably erupted in hours to days[2,6]. Such eruptions have global impacts and leave behind calderas 10–100 km in diameter as evidence of contiguous magma chambers at depth[4]. Petrologic evidence from supereruptions (>500 km^3 erupted[1]) as well as smaller recent eruptions such as Pinatubo indicates that these magma reservoirs are incrementally assembled over timescales that vary from 10^2 to 10^5 years[6–8]. Mobilization of this reservoir and eruption triggering may be caused by the injection of hot, volatile-rich, mafic magma to the base of the locked crystal mush[9,10]. However the relationship between the initiation of eruption and the pre-eruptive development of these systems remains a challenge to constrain.

Our study is motivated by the observation that many magmas from caldera-forming eruptions, such as the Fish Canyon tuff[4] and Atana ignimbrite[3], are crystal rich. Crystal fractions in these ignimbrites approach the maximum packing limit[11] where a rheological (yield stress) transition from liquid- to solid-like behaviour occurs. Many other smaller deposits have crystal fractions in the 10–30% range, in which connected networks of crystals may impart the suspension with an effective yield stress on eruptive timescales[12,13]. We focus on caldera-forming silicic eruptions because these events have a significant impact on other Earth systems[14] and because large erupted volumes minimize the nonlinear feedbacks between chamber and conduit processes exhibited by smaller silicic eruptions[15].

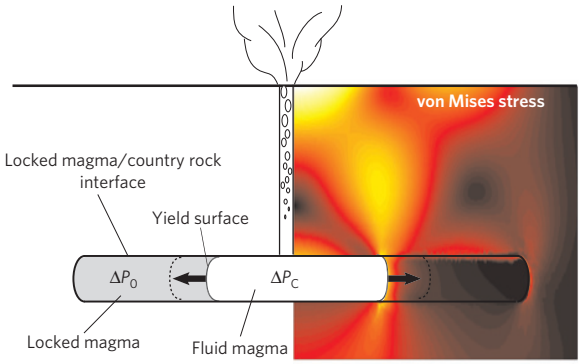

Figure 1 | The coupled conduit-flow and chamber-deformation model. Removal of magma through the conduit mobilizes locked magma in a reservoir at depth. The inner boundary of this magma chamber (the yield surface) grows in time as magma erupts, represented by an expanding cavity in an elastic half-space with overpressure ΔP_C. The outer interface between the locked magma and country rock remains fixed with initial overpressure ΔP_0. This prestressed condition generates two zones of stress concentration around the reservoir during mobilization (shaded, warm colours indicate larger von Mises stress). In this case $\Delta P_C = 10\Delta P_0$, with $\Delta P_C = 10$ MPa.

The yielding behaviour of very viscous and crystal-rich fluid has two important consequences for erupting stored magma. Foremost, it creates an evolving partition between mobile and locked portions of the magma chamber set by the position of the yield surface. Second, the yield surface maintains a difference in pore pressure between the rheologically locked and mobilized portions of the magma chamber. Thus the differential stress state on eruptive timescales (set by magma overpressure relative to lithostatic pressure) in country rocks may differ from that of locked magma, which may itself differ from mobilized magma (Fig. 1).

Overpressure develops gradually during magma-chamber construction, producing elastic stresses that grow in time unless they relax through deformation of the crust. Surface eruption is triggered once stress reaches the threshold for failure. Because elastic deviatoric stresses induced by the free surface become significant when the lateral extent of a pressurized magma chamber approaches its depth[16], calderas with lateral dimensions that exceed their depth by up to an order of magnitude (such as La Garita caldera of the Fish Canyon tuff[4]) are proxies for magma chambers that, fully mobile, would be extremely mechanically unstable. Hence we argue that it is unlikely that complete reservoir mobilization always occurs before eruption.

Department of Earth and Planetary Science, University of California, Berkeley, California 94720-4767, USA. *e-mail: leif@berkeley.edu.

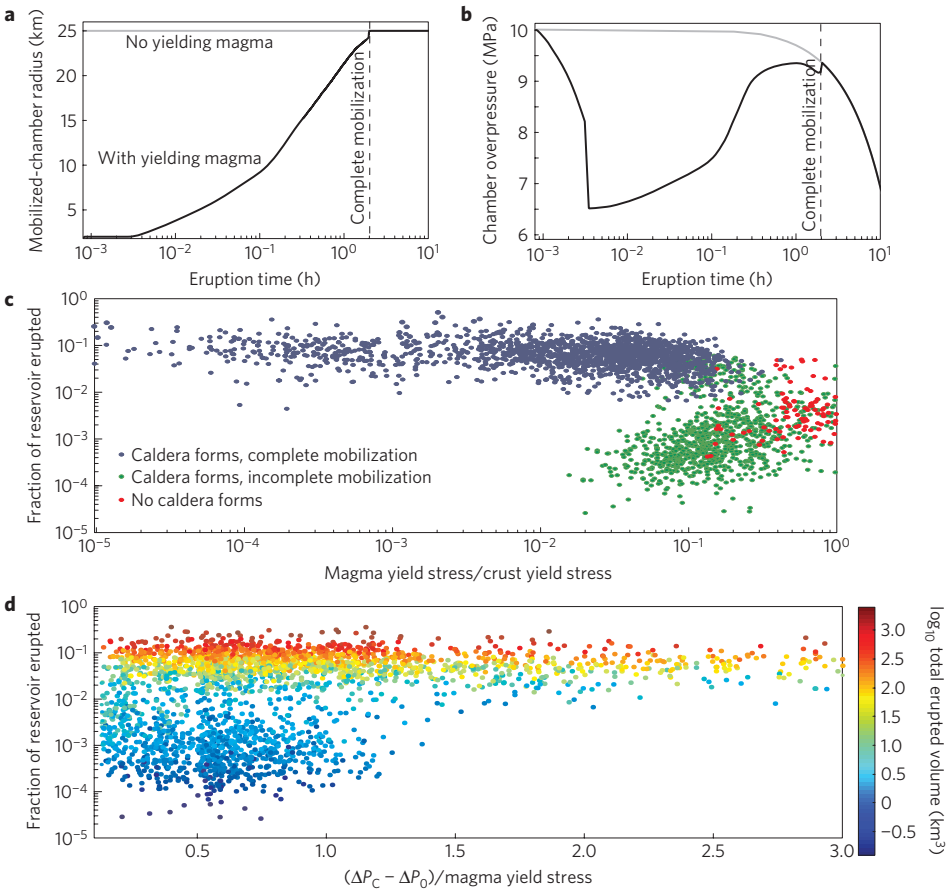

Figure 2 | Dynamics of yielding and Monte Carlo results. a, Sample evolution of chamber growth during an eruption, with (grey) and without (black) yielding magma. Locked-magma-zone radius is 25 km, conduit radius is 200 m, magma yield stress is 1 MPa, crust yield stress is 500 MPa, magma water content is 5 weight %, $\Delta P_C - \Delta P_0 = 0.1$ MPa, tenfold difference in Young's modulus between locked magma and crust. Other parameters in Supplementary Information. Initial mass flux is 13.6×10^9 kg s^{-1}. **b**, Evolution of chamber pressure. **c**, Monte Carlo results ($n = 3{,}000$), demonstrating the effect of yield stress. **d**, The effect of overpressure ($\Delta P_C - \Delta P_0$) normalized by magma yield stress for Monte Carlo results. Colour indicates $\log_{10}$ total erupted volume in km^3.

Mobilization as a result of mafic intrusion proceeds much more slowly than eruption and is prone to buoyancy instabilities[10], implying that free-surface stresses will facilitate eruption before chamber-wide mixing is complete. This is corroborated by evidence that many silicic eruptions exhibit an eruptive episode that precedes caldera collapse, often through a central vent system[17–19]. Available historical analogues also indicate that a significant fraction of the total output (>50% for Pinatubo and Katmai[20]) may be erupted before caldera formation. The syn-eruptive progression of caldera collapse into a fully mobile chamber is important after fractures decouple the caldera roof from country rocks[21]. However it does not necessarily represent the majority of erupted magma or the primary vehicle of mass transfer during many large caldera-forming eruptions.

As an alternative, we assume that some combination of rapid recharge, crystallization and volatile exsolution[22] mobilize a subset of the reservoir and pressurize it past a failure threshold, triggering eruption (Fig. 1) while much of the reservoir remains locked. Yielding then sets the progression towards caldera formation. Eruption begins with the evacuation of initially mobilized magma from a shallow, low-aspect-ratio chamber. Pressure gradients are homogenized across mobile magma by viscous flow, but low-suspension permeability and high-melt viscosity[5] maintain high pressures in locked magma. As the yield surface expands (Fig. 2a), mobilization of material buffers pressure in the fluid chamber towards its initial value (Fig. 2b). If the crustal strength is similar to the initial overpressure that triggers eruption, caldera collapse may occur during growth of the mobilized chamber as the aspect ratio and hence stress concentration increases. However, if the crust can sustain this stress accumulation around the growing chamber, all available magma will be mobilized and decompression continues until mechanical failure of the roof rocks occurs.

The eruptive dynamics predicted by this model are straightforward. Rather than exponentially decreasing discharge during decompression-controlled eruptions[23], buffering of the chamber pressure and thus discharge occurs throughout the mobilization period (Fig. 2b). Decompression and vesiculation of ascending magma induces acceleration to choked flow near the surface, so poorly known parameters of conduit flow (magma volatile content, conduit geometry, mixture viscosity) play no role in average eruption dynamics and do not affect total volume erupted. If chamber mobilization is complete or magma yield stress is large enough to allow chamber underpressure during yielding, the eruption is a siphon-like flow driven primarily by gas exsolution with a lower limit to basal pressure given by the potential energy of dissolved gas in the chamber rather than lithostatic pressure[24]. After caldera collapse begins, eruption dynamics are driven by interaction with the subsiding caldera roof[21] and are not modelled here.

Important but unknown parameters in our model include the depth and lateral extent of the locked magma reservoir, the overpressure in locked magma as well as the initial eruption-triggering pressure and the yield stresses of immobile magma and

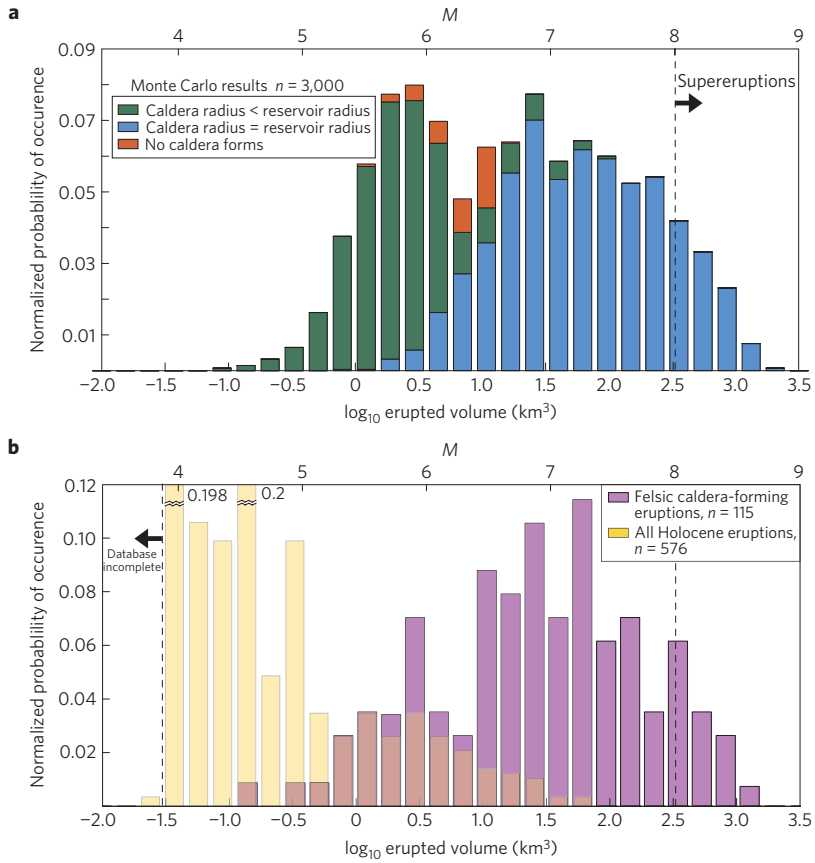

Figure 3 | Comparison of modelled eruption magnitude and frequency with available data. Sources in Supplementary Information. Bottom scale is $\log_{10}$ total erupted volume in km^3; top scale is the eruption magnitude *M*. **a**, Distribution of erupted volumes from Monte Carlo simulations. The bimodal distribution of volumes reflects whether or not the magma reservoir completely mobilizes before caldera formation. **b**, Distribution of erupted volumes from worldwide felsic collapse calderas[18] overlaid on that of all Holocene eruptions. The model distribution is similar to that observed for collapse calderas as eruption size increases. The magnitude and frequency of non-caldera-forming eruptions is distinct, with small eruptions dominant (off the scale in two cases indicated).

overlying roof rocks. Although unknown in general, constraints on these parameters come from field, laboratory and petrologic work[4,18,25]. Geometrical parameters are better constrained than evolving intensive variables such as pressure or the rheology and yielding behaviour of crystal-rich, bubbly magma. To deal with such uncertainty we assume a uniform distribution of all parameters (Supplementary Information) and carry out a suite of stochastic Monte Carlo eruption simulations. Despite this uniform prior we find a bimodal distribution of eruption volumes, reflecting caldera failure before and after the complete mobilization of locked magma (green and blue symbols in Fig. 2c). A small subset of eruptions (red symbols in Fig. 2c) end without caldera formation; in these cases, country rocks are strong enough to sustain underpressure that exceeds the potential energy available for conduit flow. Eruptions in which the magma yield stress is >1% of crust yield stress and is similar to the initial pressure difference between mobile and locked magmas exhibit caldera failure before complete mobilization (Fig. 2b–c). Other parameters do not greatly affect these results (Supplementary Fig. S3). In particular, details of our conduit-flow model do not affect the progression to caldera failure.

Long-term reservoir assembly in the shallow crust probably buffers magma crystallinity near the maximum packing fraction[26] while the reservoir grows and pressurizes, although magnitudes of magma overpressure and yield stress are uncertain. Effective yield stresses similar to stresses that trigger the eruption thus seem reasonable, augmented on eruption timescales by high stress that may endow the suspension with additional elastic strength through a jamming phase transition[27]. This implies that many caldera-forming systems fail before complete mobilization. However, volumes typical of supereruptions generally cannot be attained in this regime. The largest eruptions require strong country rocks (a critical von Mises stress of $>10^8$ Pa) and large magma-storage zones (radii of >20 km) irrespective of other parameters (Fig. 2 and Supplementary Figs S3 and S4), ending always in an underpressured state.

Our simulations generate a size distribution of caldera-forming eruptions that may be compared to the geologic record (Fig. 3). Despite model assumptions and the incomplete nature of available data, the predicted magnitude–frequency distribution is statistically similar to that derived from available data on worldwide collapse calderas (more detailed exploration of this data in Supplementary Figs S6 and S7). The distribution of large eruptions aligns best with that of completely mobilized chambers (blue bars in Fig. 3a). However, the data exhibit a more complex and multimodal distribution as erupted volume decreases. In our model, premature caldera failure leads to an increase in small eruptions as is observed in the data (Supplementary Fig. S7). We do not strive for quantitative agreement between modelled eruptions and data, as the true distribution of governing parameters is unknown. Nevertheless, similarity between modelled erupted volumes and the observational record is robust. Both modelled and real caldera distributions are distinct from that of recorded Holocene eruptions (Fig. 3b). The conditions leading to and dynamics of caldera-forming eruptions are thus not common to all volcanic eruptions.

We suggest that basic observables of caldera-forming eruptions, such as erupted volume and caldera size, reflect the natural variability of crustal strength and magma rheology. Yielding during eruption may generate calderas that do not reflect the lateral dimension of the underlying magma reservoir, leaving a significant fraction of magma locked as roof failure occurs. For caldera radii much less than that of the reservoir (Supplementary Fig. S4) residual magma may not be mobilized syn-collapse, providing a seed for future eruption and development of caldera complexes[4]. Heterogeneity of phenocryst populations and inferred differentiation times within single eruptive units observed in multicycle caldera systems[7,28] may be a consequence of similar episodic magmatic processes. Our work challenges models for silicic eruptions that require complete mobilization and chamber-wide convection before eruption triggering[10], however it does not preclude bulk chemical homogenization through the recharge-driven stirring of silicic magma reservoirs[5].

The timescale dependence of magma rheology plays a fundamental role in magma transport through the crust, as it does for controlling the style and magnitude of volcanic eruptions. This study views magma chambers dynamically, defined by a rheological transition that occurs on the timescale of eruptions. It is therefore separate from the dynamics of magma-chamber convection and from the petrologic role of these structures in facilitating magma differentiation and ascent through the crust. Such a distinction is similar in spirit to the geodynamic and geochemical definitions of the lithosphere[29] and highlights the general problem in Earth science of relating static measurements and dynamics on human timescales to inaccessible domains of time and space.

Methods

To explore the consequences of yielding rheology on eruption dynamics, we developed a numerical model that couples flow in a conduit with the evacuation of a laterally extensive but finite magma chamber located beneath a free surface. We model time-dependent magma-chamber evacuation and steady, isothermal flow through a cylindrical conduit (Fig. 1). Chamber deformation is calculated with an equation of state that relates mass removal by eruption to deformation of the (assumed elastic) surroundings. Yielding, chamber growth and roof-rock failure occur according to the von Mises criterion (Supplementary Information).

Our one-dimensional model for conduit flow contains simplified representations of the generally unsteady, multiphase fluid dynamics of volcanic eruptions[30], solving conservation equations of mass and momentum for a mixture of solid, liquid and gas. We model fragmentation of the flow and the vertical variation of apparent viscosity with water content, crystal fraction, vesicularity and strain rate (Supplementary Information). We neglect non-equilibrium bubble growth and the effects of lateral strain-rate variations in the conduit, justified as our primary focus is the coupling between magma-chamber evacuation and conduit flow. Processes that occur on magma mixing rather than much shorter eruptive timescales, such as magma recharge, are also neglected. We assume that overpressure gradually develops during magma-chamber construction, producing elastic stresses smaller than the crust-failure strength but larger than lithostatic stress. Surface eruption is then triggered by some combination of rapid recharge, crystallization and volatile exsolution[22] that mobilize a subset of the reservoir and pressurize it past a crust-failure threshold.

Received 21 November 2011; accepted 21 March 2012; published online 29 April 2012

References

1. Self, S. The effects and consequences of very large explosive volcanic eruptions. *Phil. Trans. R. Soc. A* **364,** 2073–2097 (2006).
2. Bryan, S. E. *et al.* The largest volcanic eruptions on Earth. *Earth Sci. Rev.* **102,** 207–229 (2010.).
3. Lindsay, J. M. *et al.* Magmatic evolution of the La Pacana caldera system, central Andes, Chile: Compositional variation of two cogenetic large-volume felsic ignimbrites. *J. Petrol.* **42,** 459–486 (2001).
4. Lipman, P. Incremental assembly and prolonged consolidation of Cordilleran magma chambers: Evidence from the southern Rocky Mountain volcanic field. *Geosphere* **3,** 42–70 (2007).
5. Bachmann, O. On the origin of crystal-poor rhyolites: Extracted from batholithic crystal mushes. *J. Petrol.* **45,** 1565–1582 (2004).
6. Turner, S. & Costa, F. Measuring timescales of magmatic evolution. *Elements* **3,** 267–272 (2007).
7. Druitt, T., Costa, F., Deloule, E., Dungan, M. & Scaillet, B. Decadal to monthly timescales of magma transfer and reservoir growth at a caldera volcano. *Nature* **482,** 77–80 (2012).
8. Halliday, A. N. *et al.* Evidence for long residence times of rhyolitic magma in the Long Valley magmatic system: The isotopic record in precaldera lavas of Glass Mountain. *Earth Planet. Sci. Lett.* **94,** 274–290 (1989).
9. Pallister, J. S., Hoblitt, R. P. & Reyes, A. G. A basaltic trigger for the 1991 eruptions of Pinatubo volcano? *Nature* **356,** 426–428 (1992).
10. Burgisser, A. & Bergantz, G. W. A rapid mechanism to remobilize and homogenize highly crystalline magma bodies. *Nature* **471,** 212–215 (2011).
11. Stickel, J. J. & Powell, R. L. Fluid mechanics and rheology of dense suspensions. *Annu. Rev. Fluid Mech.* **37,** 129–149 (2005).
12. Philpotts, A., Shi, J. & Brustman, C. Role of plagioclase crystal chains in the differentiation of partly crystallized basaltic magma. *Nature* **395,** 343–346 (1998).
13. Saar, M. O., Manga, M., Cashman, K. V. & Fremouw, S. Numerical models of the onset of yield strength in crystal-melt suspensions. *Earth Planet. Sci. Lett.* **187,** 367–379 (2001).
14. Rampino, M. R. & Self, S. Volcanic winter and accelerated glaciation following the Toba super-eruption. *Nature* **359,** 50–52 (1992).
15. Jaupart, C. & Allègre, C. J. Gas content, eruption rate and instabilities of eruption regime in silicic volcanoes. *Earth Planet. Sci. Lett.* **102,** 413–429 (1991).
16. Gudmundsson, A. Formation and development of normal-fault calderas and the initiation of large explosive eruptions. *Bull. Volcanol.* **60,** 160–170 (1998).
17. Self, S., Goff, F., Gardner, J., Wright, J. V. & Kite, W. M. Explosive rhyolitic volcanism in the Jemez Mountains: Vent locations, caldera development and relation to regional structure. *J. Geophys. Res.* **91,** 1779–1798 (1986).
18. Geyer, A. & Marti, J. The new worldwide collapse caldera database (CCDB): A tool for studying and understanding caldera processes. *J. Volcanol. Geotherm. Res.* **175,** 334–354 (2008).
19. Marti, J., Geyer, A., Folch, A. & Gottsmann, J. in *Studies in Volcanology: The Legacy of George Walker* (eds Thordarson, T., Self, S., Larsen, G., Rowland, S. & Hoskuldsson, A.) 249–266 (Special Publication of IAVCEI, No. 2, Geological Society, 2009).
20. Stix, J. & Kobayashi, T. Magma dynamics and collapse mechanisms during four historic caldera-forming events. *J. Geophys. Res.* **113,** B09205 (2008).
21. Kennedy, B. M., Jellinek, A. M. & Stix, J. Coupled caldera subsidence and stirring inferred from analogue models. *Nature Geosci.* **1,** 385–389 (2008).
22. Tait, S., Jaupart, C. & Vergniolle, S. Pressure, gas content and eruption periodicity of a shallow, crystallizing magma chamber. *Earth Planet. Sci. Lett.* **92,** 107–123 (1989).
23. Huppert, H. & Woods, A. The role of volatiles in magma chamber dynamics. *Nature* **420,** 493–495 (2002).
24. Druitt, T. H. & Sparks, R. S. J. On the formation of calderas during ignimbrite eruptions. *Nature* **310,** 679–681 (1984).
25. Caricchi, L. *et al.* Non-Newtonian rheology of crystal-bearing magmas and implications for magma ascent dynamics. *Earth Planet. Sci. Lett.* **264,** 402–419 (2007).
26. Dufek, J. & Bachmann, O. Quantum magmatism: Magmatic compositional gaps generated by melt-crystal dynamics. *Geology* **38,** 687–690 (2010).
27. Liu, A. J. & Nagel, S. R. Jamming is not just cool any more. *Nature* **396,** 21–22 (1998).
28. Cathey, H. E. & Nash, B. P. The Cougar Point tuff: Implications for thermochemical zonation and longevity of high-temperature, large-volume silicic magmas of the Miocene Yellowstone hotspot. *J. Petrol.* **45,** 27–58 (2004).
29. Anderson, D. Lithosphere, asthenosphere, and perisphere. *Rev. Geophys.* **33,** 125–149 (1995).
30. Gonnermann, H. & Manga, M. The fluid mechanics inside a volcano. *Annu. Rev. Fluid Mech.* **39,** 321–355 (2007).

Acknowledgements

M.L.R. is supported by a Graduate Research Fellowship from the National Science Foundation. M.M. acknowledges support from the National Science Foundation Frontiers in Earth System Dynamics and the National Aeronautics and Space Administration. We thank the Collapse Caldera Database members for maintaining the system.

Author contributions

L.K. wrote the manuscript, prepared the figures and developed the conduit-flow model. M.L.R. carried out the finite element calculations. L.K. and M.L.R. implemented the coupling between conduit flow and chamber deformation. All authors contributed to the conceptual formulation of the model and revisions to the manuscript.

Additional information

The authors declare no competing financial interests. Supplementary information accompanies this paper on www.nature.com/naturegeoscience. Reprints and permissions information is available online at www.nature.com/reprints. Correspondence and requests for materials should be addressed to L.K.